Synthesis and Properties of Conjugated Hybrid Tetrathiafulvalene Dimers

Ignacio Pérez,[†] Sheng-Gao Liu,[‡] Nazario Martín,*[,†] and Luis Echegoyen*[,‡]

Departamento de Química Orgánica, Facultad de Ciencias Químicas, Universidad Complutense, E-28040-Madrid, Spain, and Department of Chemistry, University of Miami, Coral Gables, Florida 33124

Received January 27, 2000

The synthesis of new hybrid tetrathiafulvalene (TTF) dimers (**11a**−**c**) has been carried out by a Wittig−Horner reaction of the respective phosphonate esters (**10a**−**c**) with 2-(tetrathiafulvalenylvinyl)-9,10-anthraquinone (**9**) prepared by olefination of formyltetrathiafulvalene (**7**) and the phosphonium salt of anthraquinone **8**. Electrochemical studies show that the dimers **11a**−**c** mainly retain the electrochemical properties of both TTF and the π-extended TTF components, and most importantly, intramolecular electronic interactions between the two moieties are observed by cyclic voltammetry and Osteryoung square wave voltammetry. Semiempirical PM3 calculations reveal an almost planar geometry for the TTF and the benzene ring connected through the vinyl spacer. These compounds can form stable charge-transfer complexes with 2,3-dichloro-5,6-dicyano-1,4-benzoquinone (DDQ) showing a stoichiometry of 1:3 (D:A). Attempts to electrocrystallize the dimeric donors with different counteranions are discussed.

Introduction

Since the discovery of tetriathiafulvalene (TTF) (**1a**, Chart 1) 30 years ago,[1] a great deal of work has been devoted to this molecule and some of its derivatives such as bis(ethylenedithio)tetrathiafulvalene (BEDT-TTF) (**1c**), due to the exceptional stability of the radical cations formed upon oxidation during the preparation of charge-transfer (CT) salts and/or complexes that exhibit electrically conducting and superconducting properties.[2] Other related extended π-donor analogues in which both dithiole rings are separated by a conjugated spacer have also received special attention as materials with increased dimensionality[3] or nonlinear optical (NLO) properties[4] or as small-gap semiconductors.[5] Of particular interest are the *p*-quinodimethane analogues of TTF **2**, which oxidize at lower potential due to charge delocalization and a decreased Coulombic repulsion in the dicationic state.[6] Due to these particular electronic and geometrical features, these π-extended systems (**2**) and other largely π-extended derivatives such as **3** are attractive for the preparation of new CT complexes.[7]

In contrast to the parent TTF and its derivatives that form stable radical cations, the *p*-quinodimethane analogues of TTF form stable dicationic species by reacting with electron acceptors such as tetracyano-*p*-quinodimethane (TCNQ), leading to the formation of CT complexes with interesting electrical and magnetic properties.[6]

We have recently found that π-extended TTF derivatives covalently attached to the electron-acceptor [60]-fullerene dramatically enhance the stability of the charge-separated state in the preparation of artificial photosynthetic systems.[8] The importance of these π-extended bis-(1,3-dithiole) electron donors has recently led to the systematic study of their chemical funcionalization,[9] which enables the preparation of more sophisticated electron donor TTF derivatives[10] as well as novel electroactive donor−acceptor systems.[11]

The interest in the preparation of novel modified TTFs has been also focused on dimeric TTF molecules[12] such as **4** and higher oligomers[13] as well as polymers[14] and dendrimers[15] in a search for systems displaying multistage redox behavior, which in turn affects the formation,

[†] Universidad Complutense.

[‡] University of Miami.

(1) Wudl, F.; Smith, G. M.; Hufnage, E. J. *J. Chem. Soc., Chem. Commun.* **1970**, 1453. Hünig, S.; Kiesslich, G.; Schentzow, D.; Zahradnik, R.; Carsky, P. *Int. J. Sulfur Chem. C* **1971**, *6*, 109.

(2) Williams, J. M.; Ferraro, J. R.; Thorn, R. J.; Carlson, K. D.; Geiser, H.; Wang, H. H.; Kini, A. M.; Whangbo, M.-H. *Organic superconductors (including Fullerenes)*; Prentice Hall: Englewood Cliffs, NJ, 1992.

(3) Takahasi, K.; Tomitani, K.; Ise, T.; Shirahata, T. *Chem. Lett.* **1995**, 619.

(4) Yoshida, Z.; Kawase, T.; Awaji, H.; Sugimoto, I.; Sugimoto, T.; Yoneda, S. *Tetrahedron Lett.* **1983**, *24*, 3469. Awaji, H.; Sugimoto, T.; Misaki, Y.; Kawase, T.; Yoneda, S.; Yoshida, Z. *Chem. Mater.* **1989**, *1*, 535.

(5) Khodorkovsky, V. Y.; Veselova, L. N.; Neilands, O. Y. *Khim. Geterotsikl. Soedin.* **1990**, 130; *Chem Abstr.* **1990**, *113*, 22868t. Hanse T. K.; Lakshmikantham, M. V.; Cava, M. P.; Metzger, R. M.; Becher, J. *J. Org. Chem.* **1991**, *56*, 2720. Moore, A. J.; Bryce, M. R.; Ando, D.; Hursthouse, M. B. *J. Chem. Soc., Chem Commun.* **1991**, 320. Bryce, M. R. *J. Mater. Chem.* **1995**, *5*, 1481 and references therein.

(6) (a) Yamashita, Y.; Kobayashi, Y.; Miyashi, T. *Angew. Chem., Int. Ed. Engl.* **1989**, *28*, 1052. (b) Bryce, M. R.; Moore, A. J.; Hasan, M.; Ashwell, G. J.; Fraser, A. T.; Clegg, W.; Hursthouse, M. B.; Karaulov, A. I. *Angew. Chem., Int. Ed. Engl.* **1990**, *29*, 1450. (c) Moore, A. J.; Bryce, M. R. *J. Chem. Soc., Perkin Trans. 1* **1991**, 157.

(7) Martín, N.; Sánchez, L.; Seoane, C.; Ortí, E.; Viruela, P. M.; Viruela, R. *J. Org. Chem.* **1998**, *63*, 1268.

(8) Martín, N.; Sánchez, L.; Guldi, D. M.*Chem. Commun.* **2000**, 113.

(9) Bryce, M. R.; Finn, T.; Moore, A. J. *Tetrahedron Lett.* **1999**, *40*, 3271. Martín, N.; Pérez, I.; Sánchez, L.; Seoane, C. *J. Org. Chem.* **1997**, *62*, 5690.

(10) Boulle, C.; Desmars, O.; Gautier; N.; Hudhomme, P.; Carion, M.; Gorges, A. *Chem. Commun.* **1998**, 2197.

(11) For a recent review, see: Bryce, M. R. *Adv. Mater.* **1999**, *11*, 11. Christensen, A. C.; Bryce, M: R; Batsanov, A. S.; Howard, J. A. K.; Jeppesen, J. O.; Becher, J. *Chem. Commun.* **1999**, 2433. Herranz, M. A.; Martín, N. *Org. Lett.* **1999**, *1*, 203.

(12) For a review see: Otsubo, T.; Aso, Y.; Takimiya, K. *Adv. Mater.* **1996**, *8*, 203.

(13) Becher, J.; Lau, J.; Mørk, P. Oligotetrathiafulvalenes. In *The Oligomer Approach*; Müllen, K., Wegner, G., Eds.; Wiley-VCH: Weinheim, 1998.

(14) Roncali, J. *J. Mater. Chem.* **1997**, *7*, 2307.

(15) Bryce, M. R.; Devonport, W.; Goldenberg, L. M.; Wang, Ch. *Chem. Commun.* **1998**, 945.

10.1021/jo000111g CCC: $19.00
Published on Web 05/23/2000

Chart 1

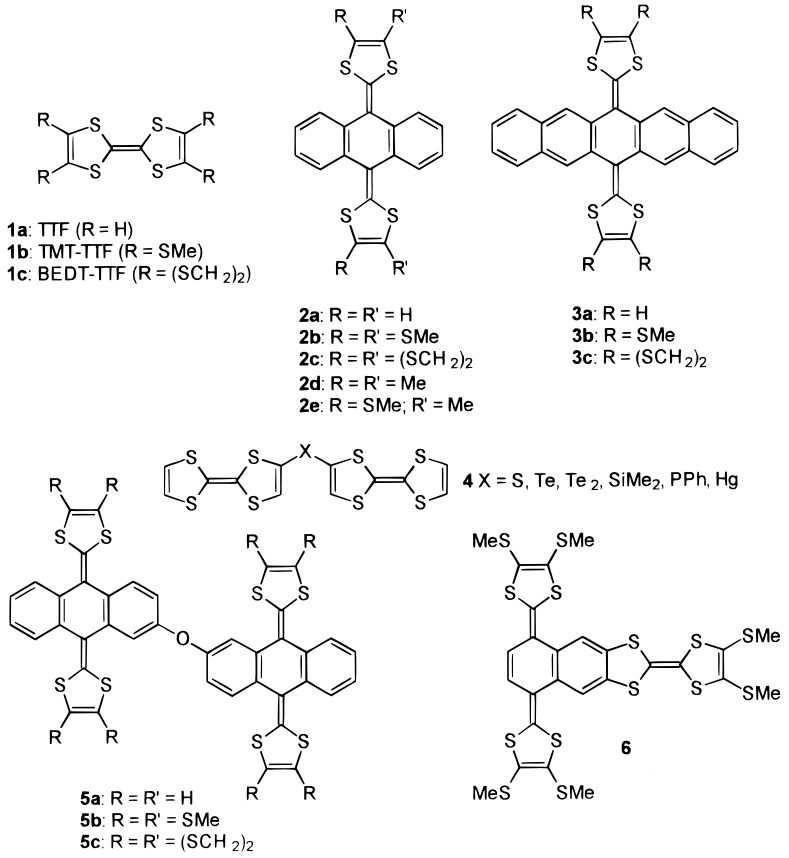

structural, and physical properties of their CT salts and/or complexes.

In contrast to the large number of studies on TTF derivatives bearing more than one TTF unit, only one recent example reporting the first dimeric TTF derivatives with quinonoid structure (**5**) is known.[16] Interestingly, the cyclic voltammetric measurements carried out on compounds **5** indicate that these dimers behave electrochemically as two independent units, showing only one, four-electron, irreversible oxidation wave at ca. 0.50 V vs SCE in CH_2Cl_2. This behavior was accounted for by the presence of the oxygen bridge, which does not allow conjugation between the two electron-donor units.

More recently, the first example of a rigid hybrid dimer formed by a TTF unit fused to a quinonoid π-extended TTF **6** has been reported by Gorgues et al.[10] Compound **6** exhibits three reversible oxidation peaks (0.27, 0.71, 1.12 V vs SCE in CH_2Cl_2). The first one corresponds to a two-electron process arising from the π-extended TTF moiety.

In this paper, we describe the synthesis, electrochemistry, spectroscopy, and complexation of hybrid electron donor systems in which the parent TTF is covalently linked to different π-electron donors containing the *p*-quinodimethane moiety through a conjugated vinyl spacer (**11a**−**c**). The presence of the double bond connecting two electroactive units serves as a bridge for the electronic interaction between them as well as for charge delocalization in the oxidized species, thus favoring the formation of CT complexes.

These novel systems are of interest as precursors for the preparation of other multichromophoric systems (dyads, tetrads, etc.) through covalent linkage to different electron acceptors. Polychromophoric systems represent one of the most important and realistic approaches in the search of photovoltaic applications.[17]

Results and Discussion

Synthesis. The preparation of the hybrid dimeric donors **11a**−**c** was carried out from formyltetrathiafulvalene (**7**)[18] and the phosphonium salt **8**[19] as shown in Scheme 1. Thus, olefination of **7** with the phosphonium salt of anthraquinone **8** under basic conditions afforded 2-(tetrathiafulvalenylvinyl)-9,10-anthraquinone (**9**) in 90% yield. Compound **9** contains the electron donor TTF conjugated with the electron acceptor 9,10-anthraquinone, and consequently, its UV−vis spectrum shows the presence of an intramolecular CT band at $\lambda_{max} = 530$ nm ($\log \epsilon = 0.72$). The latter is responsible for the violet color of this compound. In addition to the inherent nonlinear optical properties that this molecule may display, it was used as the starting material for the preparation of dimeric donors **11a**−**c** via the Wittig−Horner reaction. The carbanion was generated in situ in the presence of *n*-butyllithium from the respective phosphonate esters

(16) Martín, N.; Pérez, I.; Sánchez, L.; Seoane, P. *J. Org. Chem.* **1997**, *62*, 870.

(17) Joliffe, K. A.; Langford, S. J.; Ranasinghe, M. G.; Shephard, M. J.; Paddon-Row, M. N. *J. Org. Chem.* **1999**, *64*, 1238. See also Martín, N.; Sánchez, L.; Illescas, B.; Pérez, I. *Chem. Rev.* **1998**, *98*, 2527.

(18) Garín, J.; Orduna, J.; Moore, A. J.; Bryce, M. R.; Wegener, S.; Yufit, D. S.; Howard, J. A. K. *Synthesis* **1994**, 489.

(19) Newell, A. K.; Utley, J. H. P. *J. Chem. Soc, Chem. Commun* **1992**, 800. Listvam, V. N.; Stasyunk, A. P. *Zh. Obshch. Khim.* **1985**, *55*, 756.

Scheme 1. Synthetic Diagram of the Dimeric Donors 11a−c

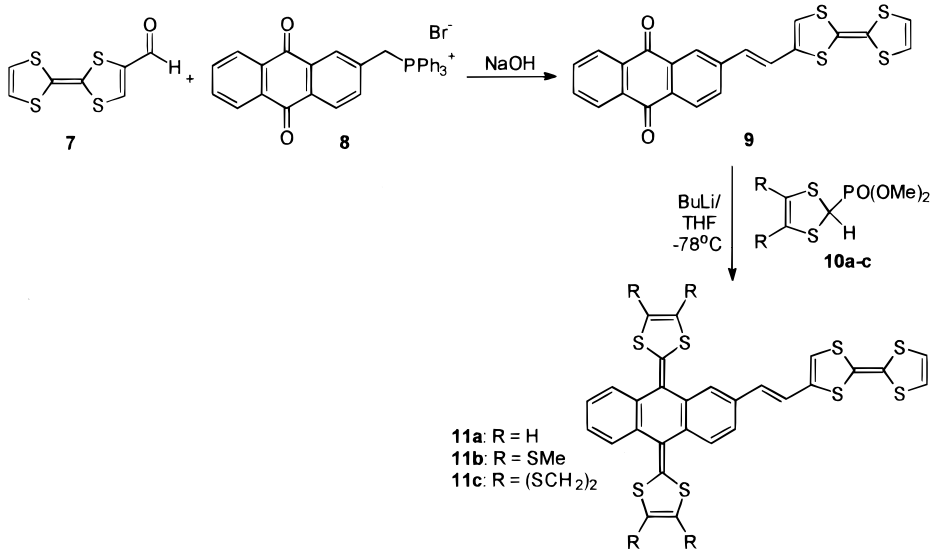

10a−c, which were in turn obtained in a multistep synthetic procedure as reported in the literature.[20] Compounds **11a−c** were obtained as stable crystalline yellow solids in good yields (57−63%) that were purified by silica gel chromatography using a hexane/methylene dichloride mixture as eluent.

The structure of the novel dimeric donors was confirmed by their analytical and spectroscopic data. The UV−vis spectra show the hypsochromic shift related to dyad **9** due to the loss of the donor−acceptor character in the dimers **11a−c**. The maxium absorption in the visible region at ca. 450 nm in CH_2Cl_2 is red-shifted when compared to that observed for the model compounds, TTF or the π-extended TTFs **2**.[6] This indicates that the two TTF moieties are conjugated and that electronic interactions exist, in very good agreement with the electrochemical analysis, as discussed below. In addition, the ^{1}H NMR spectra ($CDCl_3$, 300 MHz) demonstrate, as in **9**, the presence of only the *E* isomer in compounds **11a−c** according to the coupling constants ($J \approx 16$ Hz) of the two vinyl protons, which appear as two doublets at around 6.4 ppm (see the Experimental Section).

Electrochemistry. Solution redox properties of **11a−c** were studied by cyclic voltammetry (CV) and Osteryoung square wave voltammetry (OSWV) at ambient temperature (20 °C) and at 0 °C. Figure 1 shows the CVs of the dimers **11a−c** together with those of the model compounds TTF and the π-extended TTF derivatives **2a−c**. Anodic peak potentials (E_{pa}) for the irreversible oxidation(s) and anodic redox half-wave potentials ($E_{1/2}$) for the reversible oxidation processes are summarized in Table 1. Electrochemical data for the model π-extended TTFs (exTTFs) **2a−c**, TTF, and BEDT-TTF are also included in Table 1 for comparison.

Unlike TTF, exTTFs **2a−c** exhibit only one, two-electron, irreversible oxidation wave to form a dication. This is in good agreement with a previous report on other π-extended analogues showing only one single oxidation wave involving two electrons,[16] which was confirmed by Coulometric analysis.[6c] The coalescence of the two one-electron processes into one two-electron process reveals

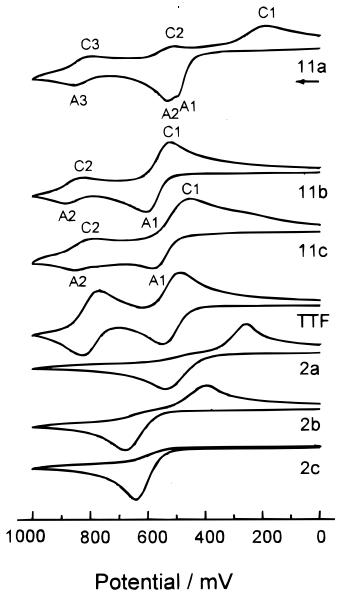

Figure 1. CVs of compounds **11a−c**, TTF, and **2a−c** in THF solution containing 0.1 M *n*-Bu_4NPF_6 with a platinum disk as the working electrode; scan from 0 to +1.0 V at 100 mV s^{-1} at room temperature.

that the presence of the quinonoid structure between the two 1,3-dithiole rings leads to unstable, highly distorted, nonplanar, radical cations. These nonplanar, unstable radical cations easily form, upon further oxidation, stable dications in which the Coulombic repulsion is remarkably decreased.[6,7] It should be pointed out that, in contrast, compound **2c** does not show any rereduction wave in the reverse scan, indicating that the dication of **2c** is extremely stable. Both **2a** and **2b** show a rereduction peak located around 260 (**2a**) and 395 mV (**2b**) at a scan rate of 100 mV s^{-1}. Furthermore, redox peak potentials are a function of the scan rate and temperature. For all three exTTFs **2a−c**, increasing the scan rate or lowering the temperature results in an increase of the oxidation peak potentials, as shown in Figure 2, suggesting that heterogeneous electron transfer is slow. In fact, low-temperature measurements show that all compounds become more difficult to oxidize, and the corresponding rereduc-

(20) Bryce, M. R.; Moore, A. J. *Synthesis* **1991**, 26. Parg, R. P.; Kilburn, J: D.; Ryan, T. G. *Synthesis* **1994**, 195 and references therein.

Table 1. E_{pa} or $E_{1/2}$[a,b] Values (mV vs Ag/AgCl) of Compounds 11a−c, TTF (1a), BEDT-TTF (1c), and 2a−c Detected by CV in THF Solution at Room Temperature Using Pt Working Electrode

compd	E_{pa}[c]	$E_{1/2}$ (ΔE_p/mV)
11a	494 (A_1), 529 (A_2)	840 (39)
11b	607 (A_1)	856 (53)[d]
11c	583 (A_1)	832 (42)[d]
TTF	519 (63)[d]	801 (52)[d]
2a	537	
2b	680	
2c	642	
BEDT-TTF	695 (56)[d]	861 (47)[d]

[a] Errors for E_{pa} or $E_{1/2}$ values are estimated at about ±5 mV. [b] $E_{1/2} = (E_{pa} + E_{pc})/2$, E_{pa}, or E_{pc}: peak potentials, $\Delta E_p = E_{pa} - E_{pc}$. [c] Peak potentials reported, due to electrochemical or chemical irreversibility. [d] $E_{1/2}$ and ΔE_p values.

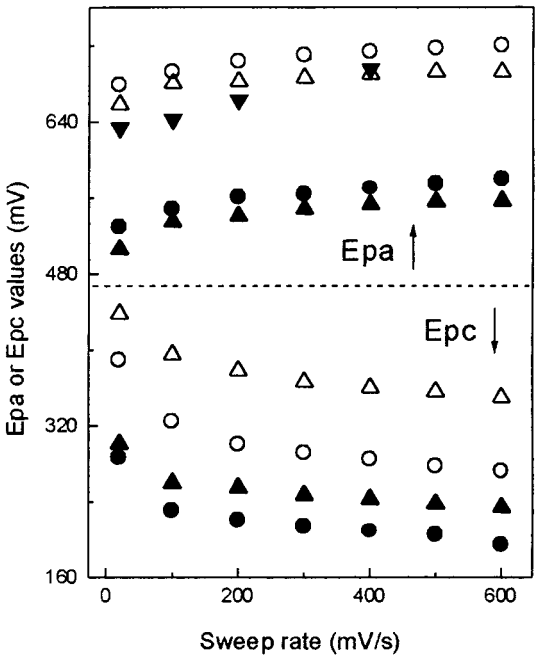

Figure 2. Sweep rate dependence of E_{pa} (upper) and E_{pc} (bottom) values for **2a** (solid), **2b** (hollow), and **2c** (down-triangle) at room temperature (triangle) and 0 °C (circle).

tion peaks **2a**,**b** in the reverse scan are shifted to more negative potentials (Figure 2). Hence, the overall effect of lowering the temperature and increasing the scan rate is to increase the ΔE_p values, as clearly shown in Figure 3. The oxidation peak potential differences between room temperature (20 °C) and 0 °C are 16, 28, and 64 mV for **2a**−**c**, respectively, as determined by OSWV.

The CVs of all three dimers **11a**−**c** show several common features. All of the compounds essentially retain the electronic properties of both the TTF and the π-extended TTF portions, exhibiting oxidation to the mono- and/or dicationic states even though their CVs are different from that of a typical TTF. As shown in Figure 1 in THF solution, between 450 and 650 mV all three dimeric donors exhibit one or two electrochemically reversible or irreversible oxidation process(es) associated with one or two rereduction process(es) between 550 and 150 mV in the reverse scan. All the dimers exhibit a reversible oxidation at ca. 850 ± 10 mV with small ΔE_p values (≤53 mV, v = 100 mV s^{-1}), and these are almost independent of either sweep rate or temperature. It is evident that this reversible oxidation corresponds to a

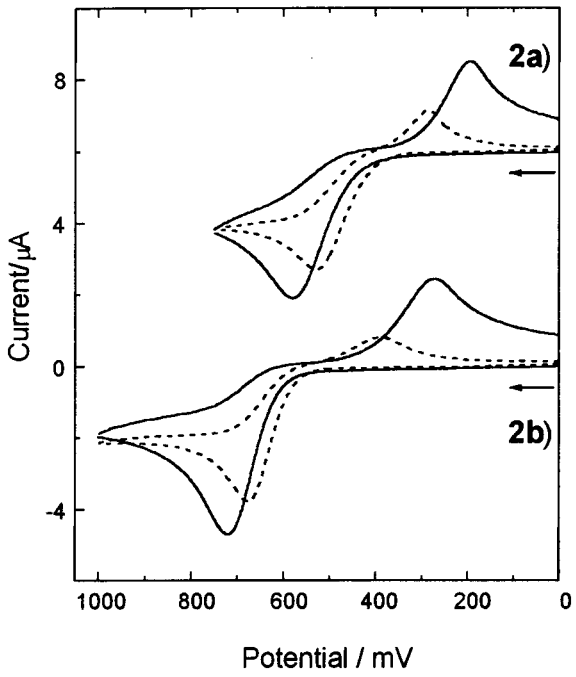

Figure 3. CVs of **2a** (upper) and **2b** (bottom) at 0 °C with scan rate of 20 (dashed) and 600 mV s^{-1} (solid). The current of **2a**,**b** at 600 mV s^{-1} was divided by 4.

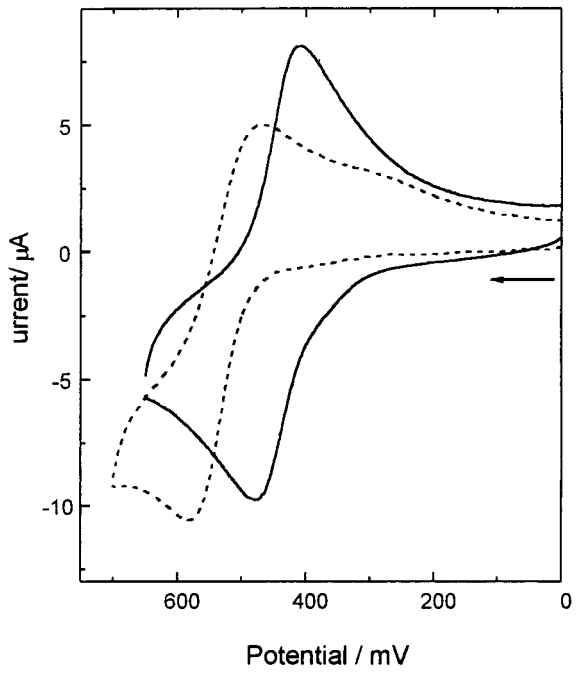

Figure 4. CVs of the first 3 e^- oxidation processes of **11c** in CH_2Cl_2 (solid) and THF (dashed) at a scan rate of 100 mV s^{-1} at room temperature.

one-electron process when compared to the corresponding oxidation of either TTF or BEDT-TTF under identical concentrations and experimental conditions. The latter have two, one-electron, reversible processes corresponding to the formation of mono- and dicationic species. In general, the CVs are solvent dependent. For example, as shown in Figure 4, the first three-electron oxidations of **11c** in CH_2Cl_2 are reversible (ΔE_p = 61 mV), but irreversible in THF (ΔE_p = 100 mV). It should be mentioned that all attempts to separate the three-electron oxidation wave between 450 and 650 mV into

two or three peaks by either lowering the scan rate, lowering the temperature, and/or changing the solvent (THF, CH_2Cl_2, CH_3CN) were not successful. A better resolution was obtained for **11a** in THF solution, which shows two oxidation waves between 450 and 650 mV (Figure 1). Due to the poor resolution between the two oxidation peaks, it is impossible to calculate the number of electrons involved in each process by either integration or controlled potential electrolysis. However, comparing the CV of **11a** with those of TTF and **2a**, one can guess that the first wave is probably a two-electron oxidation process of the π-extended TTF moiety from the neutral to the dicationic state (TTF-exTTF → TTF-exTTF^{2+}) and the second one is a one-electron reversible oxidation of the TTF moiety from the neutral to the radical cationic state (TTF-exTTF^{2+} ⇄ TTF$^{+\cdot}$-exTTF^{2+}, as detailed below). The voltammetric peak currents of all redox processes for all species **11a**−**c** are almost directly proportional to the square root of the scan rate, suggesting diffusion-controlled processes. However, the redox processes between 150 and 650 mV have anodic and cathodic peak potentials that are slightly dependent on the sweep rate, suggesting slow electron-transfer processes. For example, the cathodic peak potentials at around 200 mV (Figure 1) for **11a** and **11c** are negatively shifted as the sweep rate is increased, by 76 and 18 mV, respectively, as the scan rate is increased from 100 to 600 mV s^{-1}. This may be due to the effect of the exTTF moiety because the oxidation process(es) in this potential region are mainly exTTF-based (see below).

Considering the fact that compounds **11a**−**c** contain two different types of TTF moieties, it is important to determine which moiety is easier to oxidize. Thus, a careful comparison was made between the electrochemical data of **11a**−**c** and those of TTF and the π-extended TTFs **2a**−**c** (Figure 1 and Table 1). As can be seen in Figure 1, the π-extended TTF model compounds **2a**−**c** behave electrochemically quite different from TTF, exhibiting a one, two-electron, irreversible oxidation process associated with (for **2a**,**b**) or without (for **2c**) a rereduction peak in the reverse scan between 1.0 and 0 V. Comparing the first oxidation peak potential of TTF (550 mV) to those of **2a**−**c** shows that **2b** and **2c** are more difficult to oxidize while **2a** is slightly easier to oxidize than TTF. On the other hand, when comparing the potentials of BEDT−TTF with those of **2b** and **2c**, the latter are easier to oxidize. Hence, the E_{pa} values follow the trend **2a** < TTF < **2c** < **2b** < BEDT−TTF. This trend seems to be in good agreement with the degree of conjugation. That is, the parent TTF is less conjugated than the π-extended TTF **2a** and BEDT−TTF is less conjugated than the π-extended and substituted TTF **2b**,**c**. Therefore, in the case of compound **11a**, the first oxidation can be assigned to the π-extended TTF moiety. Considering the fact that model compound **2a** exhibits one, two-electron, irreversible oxidation process, this oxidation peak in **11a** must be a two-electron process corresponding to the formation of the dication from the neutral state. So the second oxidation process involves only one electron and should arise from the first oxidation of the TTF moiety. This explanation is in good agreement with the fact that the integration of C_2 is almost equal to that of C_3 (Figure 1). In the cases of **11b**,**c**, the first reversible (**11b**, ΔE_p = 76 mV, ν = 100 mV s^{-1}) or irreversible (**11c**, ΔE_p = 100 mV, ν = 100 mV s^{-1}) three-electron oxidation processes must be originating from

Scheme 2. Schematic Diagram of the Redox Processes for Compounds 11a−c

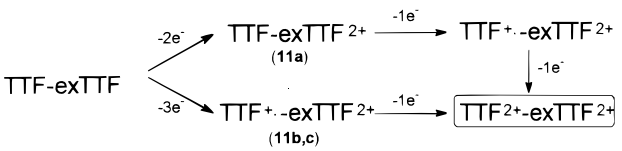

both the two-electron oxidation of the π-extended TTF moiety and the first one-electron oxidation of the TTF moiety forming a tri-cation, TTF$^{\cdot+}$−exTTF^{2+}. In summary, the oxidation process(es) between 450 and 650 mV for **11a**−**c** are both TTF and π-extended TTF-based, but the reversible, one-electron redox wave at about 850 mV ($E_{1/2}$ values) is only TTF-based, leading to the formation of a tetra-cationic state TTF^{2+}−exTTF^{2+}, as outlined in Scheme 2.

In addition, as can be observed in Figure 1 and Table 1, the first anodic oxidation peak potentials of compound **11b** are more positive than those of compound **11c**, and those of **11c** are more positive than those of **11a**, following the trend of **11a** < **11c** < **11b**. This indicates that the first oxidation of the extended TTF moiety in **11b** is more difficult than that of **11c** and that of **11c** is more difficult than that of **11a**. This is in perfect agreement with the electrochemical data of the model exTTFs **2a**−**c** (see above) and of TTF (**1a**), BEDT−TTF (**1c**), and TMT−TTF (**1b**) [tetra(methylthio)-tetrathiafulvalene] (**1a** < **1c** < **1b**).[21]

Thus, the geometric distortion found in the exTTFs **2a**−**c** could be responsible for the coalescence of the first and second oxidation processes, typical of TTF derivatives, into a single two-electron oxidation wave to form a planar, aromatic hydrocarbon skeleton in **11a**−**c**.[16] Although the same trend was observed in THF for compounds **11a** and **11c**, this is not the case for **11b**, which showed a reversible oxidation wave (ΔE_p = 76 mV at 100 mV s^{-1}) as is shown in Figure 1. This behavior is consistent with that observed for **5a**−**c**.[16]

Interestingly and most importantly, when comparing the CVs of the dimeric TTF donors **11a**−**c** with those of the model compounds TTF and exTTFs **2a**−**c**, although some common features exist it is also quite obvious that in each case the CV of the dimeric TTF is not exactly the sum of the CVs of TTF and exTTF. This is a good indication of intramolecular electronic interactions between the two donor moieties.

As can be seen in Table 1, all TTF-based reversible, one-electron oxidation waves at about 850 mV ($E_{1/2}$ values) for **11a**−**c** are more positive than the second one-electron oxidation process of TTF (TTF$^{\cdot+}$ ⇄ TTF^{2+}, $E_{1/2}{}^2$ = 801 mV) by about 30−55 mV. This indicates the existence of intramolecular electronic interactions between the two different TTF moieties in the charged states of **11a**−**c**, i.e., when they are oxidized from the neutral to the tri-cationic state (TTF$^{\cdot+}$−exTTF^{2+}), the second oxidation of the TTF moiety becomes more difficult due to the electron withdrawing effect of the positively charged dication state of the exTTF moiety. Such an intramolecular electronic interaction is also observed in the ground state. Thus, a comparison of the first oxidation potentials of **11a**−**c** (TTF−exTTF → TTF−exTTF^{2+}) with those of the model exTTFs **2a**−**c** (Table

(21) Liu, S.-G.; Liu, Y.-Q.; Wu, P.-J.; Li, Y.-F.; Zhu, D.-B. *Phosphorus, Sulfur, Silicon* **1997**, *127*, 81−89.

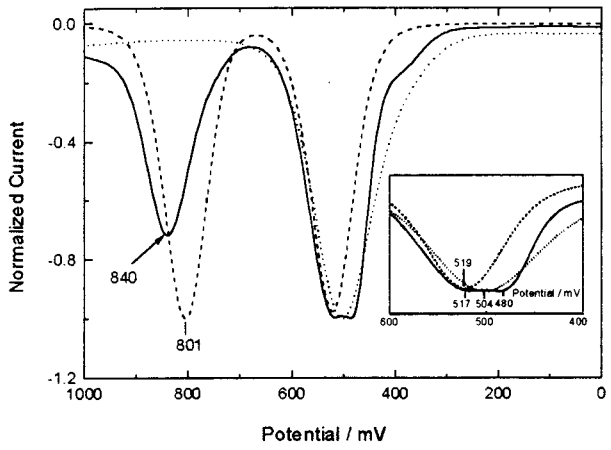

Figure 5. OSWVs of compounds **11a** (solid), **TTF** (dashed), and **2a** (dotted) in THF solution containing 0.1 M *n*-Bu_4NPF_6 at room temperature.

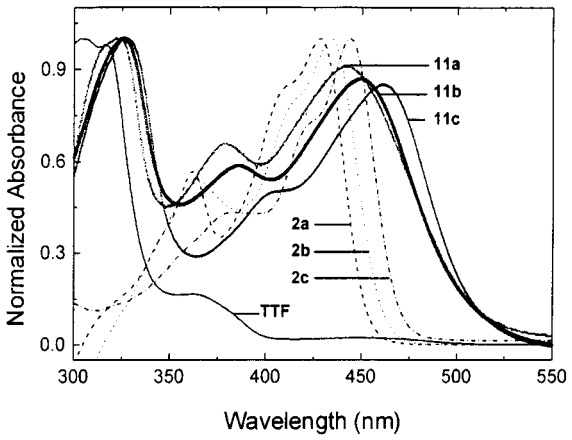

Figure 6. UV−vis spectra of TTF, **2a**−**c** and **11a**−**c** in THF at room temperature.

1), reveals that the anodic peak potential differences for **2a**−**11a**, **2b**−**11b**, and **2c**−**11c** are about 43, 73, and 59 mV, respectively. This can be easily explained by the conjugation effect between the two donor moieties. In addition, considering this conjugation effect, the first oxidation of the TTF moiety in **11a**−**c** should be more negative than that of the parent TTF. However, when the exTTF moiety was initially oxidized to the dicationic state, the first oxidation of the TTF moiety became more positive. So, the overall effect is small on the first oxidation of the TTF moiety in **11a** with respect to the parent TTF, clearly visible in the OSWV (Figure 5). This supports our assignment of the first two nearly coalesced oxidations of **11a**. Such a ground-state intramolecular electronic interaction is in very good agreement with the UV−vis spectroscopic analysis. As shown in Figure 6, the UV−vis spectra of **11a**−**c** in THF are mainly dominated by the absorption of both TTF moiety in the UV region and exTTF moiety in the visible region. Thus, a comparison of the λ_{max} values between 300 and 350 nm shows a red-shift of 6, 9, and 11 nm for **11a**−TTF, **11b**−TTF, and **11c**−TTF, respectively, and between 400 and 550 nm, a red shift of 15, 16, and 19 nm was observed for **11a**−**2a**, **11b**−**2b**, and **11c**−**2c**, respectively.

It should be pointed out that such an intramolecular electronic interaction observed in **11a**−**c** is in contrast with observations of the dimers **5a**−**c**, in which the two donor fragments behave independently, showing only one, four-electron, irreversible oxidation wave.[16] The spacer C=C double bond between the two TTF moieties could account for this difference. Since the two π-extended TTF moieties in **5a**−**c** were connected via an oxygen atom, electronic coupling is inhibited. However, the intramolecular electronic interactions observed for **11a**−**c** are consistent with observations for **4**, which showed a negligible through-space and through-bond orbital interactions between the two TTF units.[22]

Charge-Transfer Complexes or Salts. Despite the strong electron-donating ability of the dimeric donors **11a**−**c** as determined by CV, they did not form CT complexes with acceptors such as TCNQ or DCNQI, suggesting that geometrical factors may play a significant role on the complexation process. However, **11a**−**c** form stable CT complexes with stronger electron acceptors such as dichlorodicyano-*p*-benzoquinone (DDQ). Thus, a boiling solution of **11a**−**c** in dry methylene dichloride was mixed with DDQ under an argon atmosphere and a dark solution was formed. The dark solid precipitated was collected by filtration and washed with cold CH_2Cl_2. The complexes obtained show the presence of the characteristic CT-bands in the visible region of the electronic spectra (**11a**: 588 nm; **11b**: 590 nm; **11c**: 588 nm).

All complexes showed a 1:3 (D/A) stoichiometry by elemental analyses. These results are similar to those found for the CT-complexes prepared from **5a**−**c**.[16] The vibrational frequencies (FTIR) of the C≡N groups in the complexes confirm the absence of the dianion of DDQ in the CT-complexes (DDQ^{2-}: 2192, 2169 cm^{-1}).[23]

In addition, attempts were made to grow CT salts by electrocrystallization under different conditions (concentration, current, and/or solvent) of donors **11** with different counteranions, such as PF_6^-, BF_4^-, and I_3^-.[2] However, all of our efforts to grow single crystals with **11a**−**c** were unsuccessful. In most cases, a black powder was formed on the surface of the anode. Two-probe powder electrical conductivity measurement on the compressed pellets of these CT salts showed the conductivity to be less than 1×10^{-6} S cm^{-1}, which may account for the difficulty to grow single crystals.

Molecular Structure. The molecular structure of compound **11a** has been optimized by using semiempirical calculations at the PM3 level. It has been previously reported that the theoretical calculations carried out for compounds **2** show a good agreement between theory and experiment and demonstrate that the PM3 method provides a good description, even better than ab initio HF/6-31G* calculations, of the molecular structure of extended TTFs.[7]

As shown in Figure 7 two minimum-energy conformations of **11a** (A and B) were found with an energy difference of ~0.5 kcal/mol. As expected, the TTF moiety shows a planar structure and the π-extended TTF presents a butterfly-shaped nonplanar geometry. The planar conformation of the π-extended TTF moiety is strongly hindered by the short distance between the peri hydrogens and the sulfur atoms (1.78 Å). To avoid these interactions, the molecule is distorted out of planarity with the central ring in a boat conformation (distance S···H, 2.62 Å).

Distortions from planarity can be described in terms of the angles α and γ. Angle α corresponds to the angle

(22) Formigué, M.; Huang, Y.-S. *Organometallic* **1993**, *12*, 797.
(23) Miller, J. S.; Dixon, D. A. *Science* **1987**, *235*, 871.

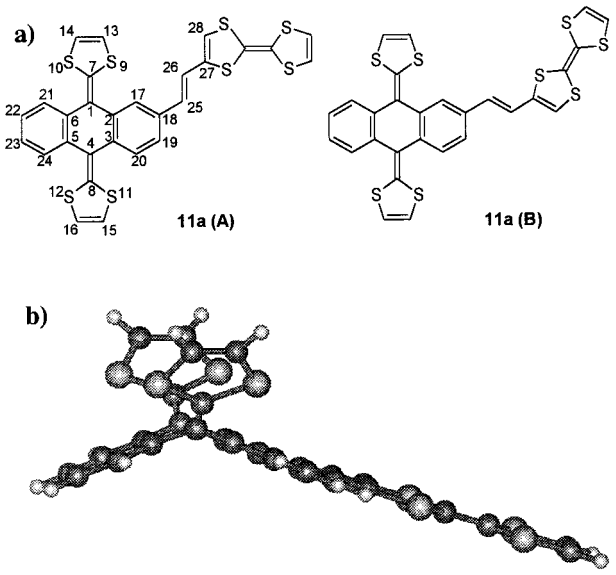

Figure 7. (a) Minimum energy conformations (A and B) calculated by PM3 for compound **11a**. An aleatory atom numbering is used in the text. (b) Butterfly-shaped minimum-energy conformation (A) calculated for **11a** showing the planarity of the vinyl spacer with the TTF moiety.

formed by the outer benzene rings (the wings of the butterfly), and γ defines the tilting of the dithiole units and is obtained as the supplement of the C7−C2−C6−C5 dihedral angle. These calculated angles ($\alpha = 141.5°$ and $\gamma = 36.0°$) for the more stable conformation **11a** (A) are in good agreement with that observed for compound **2b** in the crystal[6b] ($\alpha = 143.8°$ and $\gamma = 33.3°$) as well as for those obtained by theoretical calculations for compounds **2**[7] (PM3: $\alpha = 139.0°$ and $\gamma = 34.8°$; HF/6-31G*: $\alpha = 136.3°$ and $\gamma = 39.4°$; B3-P86/6-31G*: $\alpha = 142.1°$ and $\gamma = 34.0°$).

Figure 7b shows the planarity of the vinyl-TTF moiety which presents a dihedral angle C18−C25−C26−C27 of 177.8° with the benzene fused ring to the π-extended TTF moiety (dihedral angle C17−C18−C25−C26 = 2.38° and C25−C26−C27−C28 = 178.10°). These data confirm that both TTF and π-extended TTF units are in conjugation through the vinyl spacer, thus supporting the electrochemical findings.

Conclusions

The synthesis of novel conjugated TTF dimers **11a**−**c** was reported by the Wittig−Horner reaction of the respective phosphonate esters (**10a**−**c**) with 2-(tetrathiafulvalenylvinyl)-9,10-anthraquinone (**9**). Electrochemical studies of these new hybrid TTF dimers **11a**−**c** show that they retain the electronic properties of both TTF and π-extended TTF moieties with successive oxidations from neutral to mono- and/or dication states. The initial oxidation process originates from the π-extended TTF moiety rather than from the TTF moiety. Careful analysis by either CV or OSWV indicates that for dimer **11a** successive electrochemical oxidations correspond to a two-, one-, one-electron process while for **11b** and **11c** it is a three-, one-electron sequence. Intramolecular electronic interactions between the two different TTF moieties are evident both for the neutral as well as for the charged states upon successive electrochemical oxidations. Semiempirical PM3 calculations reveal an almost planar geometry for the TTF and the benzene ring connected through the vinyl spacer.

Experimental Section

General Instrumentation and Descriptions. All chemicals were of reagent grade. All solvents were dried over molecular sieves (4 Å) and purified according to standard procedures prior to use. All temperatures quoted were uncorrected. Column chromatography was performed on silica gel (230−240 mesh). Mass spectra were recorded in the positive FAB mode using *N*-bromoacetamide (NBA) as the matrix.

Cyclic voltammetry (CV) and Osteryoung square wave voltammetry (OSWV) were performed at room temperature and at 0 °C with a three-electrode configuration in THF solution containing the substrate (0.5−1.0 mM) and a supporting electrolyte. A platinum (∅ 1 mm) disk served as the working electrode, a platinum wire (∅ 1 mm) and a commercial Ag/AgCl aqueous electrode being the counter and the reference electrodes, respectively. Both the counter and the reference electrodes were directly immersed in the electrolyte solution. THF was dried over sodium and purified by distillation from sodium and benzophenone prior to use. Tetrabutylammonium hexafluorophosphate (n-Bu_4NPF_6) (>99%) was recrystallized twice from ethanol and dried in a vacuum overnight prior to use and was employed as the supporting electrolyte in 0.1 M concentration. Solutions were stirred and deaerated by bubbling argon for a few minutes prior to each voltammetric measurement. Scan rate was 100 mV s^{-1} unless otherwise specified. OSWVs were obtained using a sweep width of 25 mV, a frequency of 15 Hz, a step potential of 4 mV, a S. W. amplitude of 25 mV, and a quiet time of 2 s.

Electrocrystallization was attempted at room temperature by using standard U-type cells equipped with a sintered glass filter plate in the middle and two Pt electrodes (∅ 1 mm) in both the anodic and cathodic compartments. The donor molecule was placed in the anodic compartment and dissolved in an appropriate solvent (CH_2Cl_2 or chlorobenzene). $TBAPF_6$, $TBABF_4$, or $TBAI_3$ (TBA = tetrabutylammonium) was placed in both compartments of the U-type cell serving as the supporting electrolyte and the counteranion. The current employed was generally around 0.1−1.0 μA for a period of 2−30 days.

2-(2-Tetrathiafulvalenylvinyl)-9,10-anthraquinone (9). To a suspension of the phosphonium bromide **8** (1.0 mmol) and formyl-TTF **7** (1.0 mmol) were added 30 mL of CH_2Cl_2 and 1.0 mL of NaOH (1.0 N) aqueous solution. An emerald-green color appeared, and the solution was gently stirred until the green color of the phosphorane disappeared. The organic layer was separated, washed with water, and dried, and the solvent was removed under reduced pressure. The resulting mixture was then purified by silica gel chromatography using hexane/ethyl ether (2:1) as the eluent, and a green solid (violet in solution) was obtained in 90% yield: ^{1}H NMR ($CDCl_3$; 300 MHz) δ 6.36 (2H, s), 6.48 (1H, d, J = 15.6 Hz), 6.58 (1H, s), 7.16 (1H, d, J = 15.3 Hz), 7.76 (1H, dd, J_1 = 8.4 Hz, J_2 = 2.5 Hz), 7.81 (2H, m) 8.28 (1H, d, J = 8.1 Hz), 8.33 (3H, m); ^{13}C NMR ($CDCl_3$; 75 MHz) δ 124.9, 127.2, 127.7, 132.0, 133.4, 133.5, 134.1, 134.2, 147.6, 163.7, 170.1; FTIR (KBr) 1671, 1587 cm^{-1}; MS m/z 436 (M^+); UV−vis (CH_2Cl_2) λ_{max} (nm) (log ϵ) 256 (1.78), 280 (1.77), 368 (1.28), 530 (0.72). Anal. Calcd for $C_{22}H_{12}O_2S_4$: C, 60.53; H, 2.77. Found: C, 59.96; H, 2.41.

General Procedure for the Synthesis of Hybrid Dimers 11a−c. To a solution of the corresponding 1,3-dithiolylphosphonate **10** (1.5 mmol) in dry THF (10 mL) was dropwise added 1.0 mL of n-BuLi (1.6 M in hexane) under argon atmosphere. The resulting solution was stirred at −78 °C for 30 min. A suspension of **9** (0.3 mmol) in dry THF (10 mL) was then added and kept under these conditions for an additional 1 h and then at room temperature overnight. The solvent was removed under reduced pressure, and the residue washed with water and extracted with CH_2Cl_2. The organic layer was dried, and the solvent was removed under reduced pressure. The resulting solid was purified by silica gel chromatography using hexane/methylene dichloride as the eluent.

2-(2-Tetrathiafulvalenylvinyl)-9,10-bis(1,3-dithiol-2-ylidene)-9,10-dihydroanthracene (11a): 57% yield; mp 160−162 °C; ^{1}H NMR ($CDCl_3$; 300 MHz) δ 6.31 (4H, s), 6.34 (2H, s), 6.39 (1H, s), 6.43 (1H, d, J = 15.8 Hz), 6.91 (1H, d, J = 15.8 Hz), 7.30 (3H, m), 7.68 (3H, m), 7.74 (1H, d, J = 1.74 Hz); ^{13}C NMR ($CDCl_3$; 75 MHz) δ 117.1, 117.3, 118.5, 119.0, 119.1, 120.1, 122.7, 124.3, 124.9, 125.3, 126.0, 131.7, 134.0, 135.2, 135.8, 136.1, 136.7; FTIR (KBr) 1544, 1509 cm^{-1}; UV−vis (CH_2Cl_2) λ_{max} (nm) (log ϵ) 238 (1.84) 316 (1.87), 380 (1.66), 442 (1.71); MS m/z 607.9 (M^+); HRMS m/z found 607.9018, calcd for $C_{28}H_{16}S_8$ 607.9018.

2-(2-Tetrathiafulvalenylvinyl)-9,10-bis(4,5-dimethylthio-1,3-dithiol-2-ylidene)-9,10-dihydroanthracene (11b): 63% yield; mp 148−150 °C; ^{1}H NMR ($CDCl_3$; 300 MHz) δ 2.40 (12H, s), 6.35 (2H, s), 6.42 (1H, d, J = 15.7 Hz), 6.43 (1H, s), 6.92 (1H, d, J = 15.8 Hz), 7.32 (3H, m), 7.52 (1H, d, J = 8.0 Hz), 7.60 (3H, m); ^{13}C NMR ($CDCl_3$; 75 MHz) δ 19.2, 118.9, 119.0, 120.7, 123.3, 124.4, 125.3, 125.4, 125.8, 126.4, 131.3, 131.4, 134.3, 134.4, 135.1, 135.9, 136.8; FTIR (KBr) 1529, 1495 cm^{-1}; UV−vis (CH_2Cl_2) λ_{max} (nm) (log ϵ) 244 (2.14), 326 (2.02), 388 (1.81), 446 (1.98); MS m/z (FAB$^+$) 791.9 (M^+); HRMS m/z found 791.8525, calcd for $C_{32}H_{24}S_{12}$ 791.8527.

2-(2-Tetrathiafulvalenylvinyl)-9,10-bis(4,5-ethylenedithio-1,3-dithiol-2-ylidene)-9,10-dihydroanthracene (11c): 58% yield; mp > 300 °C;^{1}H NMR ($CDCl_3$; 300 MHz) δ 3.31 (8H, s), 6.35 (2H, s), 6.43 (1H, s), 6.44 (1H, d, J = 16.2 Hz), 6.92 (1H, d, J = 15.3 Hz), 7.33 (3H, m), 7.48 (1H, d, J = 9.6 Hz), 7.51 (3H, m); ^{13}C NMR ($CDCl_3$; 75 MHz) δ 29.6, 111.0, 118.9, 119.0, 120.7, 123.8, 124.6, 125.5, 126.4, 131.4, 134.5, 136.0, 136.7, 136.8; FTIR (KBr) 1507, 1450 cm^{-1}; UV−vis (CH_2Cl_2) λ_{max} (nm) (log ϵ) 234 (1.82), 324 (1.65), 406 (1.37), 458 (1.56); MS m/z (FAB$^+$) 787.8 (M^+), 307.1, 154.1; HRMS m/z found 787.8214, calcd for $C_{32}H_{20}S_{12}$ 787.8214.

General Procedure for the Preparation of CT Complexes. To a boiling solution of the corresponding donor (**11**) (0.010 mmol) in dry CH_2Cl_2 (10 mL) was added a solution of the acceptor DDQ (0.040 mmol) in dry CH_2Cl_2 (5 mL) under argon atmosphere and kept under these conditions for 30 min. The resulting dark solution was filtered, and a dark solid was collected, washed with cold CH_2Cl_2, and dried in vacuo to afford the corresponding CT complexes.

11a:(DDQ)$_3$:(CH$_2$Cl$_2$)$_2$: 32% yield; FTIR (KBr) 2223 (C≡N), 1559 cm^{-1}; UV−vis (CH_3CN) λ_{max} (nm) 202, 256, 346, 418, 588. Anal. Calcd for $C_{54}H_{20}N_6Cl_{10}O_6S_8$: C, 44.43; H, 1.38; N, 5.76. Found: C, 44.65; H 1.68; N, 5.82.

11b:(DDQ)$_3$:(CH$_2$Cl$_2$): 29% yield; FTIR (KBr) 2210 (C≡N), 1559 cm^{-1}; UV−vis (CH_3CN) λ_{max} (nm) 218, 258, 344, 418, 590. Anal. Calcd for $C_{57}H_{26}Cl_8N_6O_6S_{12}$: C, 43.91; H, 1.68; N, 5.39. Found: C, 44.05; H, 1.89; N, 5.47.

11c:(DDQ)$_3$:CH$_2$Cl$_2$: 35% yield; FTIR (KBr) 2225 (C≡N), 1560 cm^{-1}; UV−vis (CH_3CN) λ_{max} (nm) 220, 338, 458, 588. Anal. Calcd for $C_{57}H_{22}Cl_8N_6O_6S_{12}$: C, 44.02; H, 1.43; N, 5.40. Found C, 43.91; H, 1.73; N, 5.60.

Acknowledgment. Financial support by the Fullbright Foundation (Project 99125). I.P. and N.M. gratefully acknowledge the DGESIC of Spain (Project PB98-0818). S.-G.L. and L.E. greatly appreciate the National Science Foundation, grant CHE-9803088, for generous support of this work.

JO000111G